Accuracy of 4 Different Algorithms for the Analysis of Tomographic Radionuclide Ventriculography Using a Physical, Dynamic 4-Chamber Cardiac Phantom

Pieter De Bondt, MD[1,2]; Tom Claessens MScCivE[3]; Bart Rys[3]; Olivier De Winter, MD[1]; Stijn Vandenberghe, PhD[3]; Patrick Segers, PhD[3]; Pascal Verdonck, PhD[3]; and Rudi Andre Dierckx, MD, PhD[1]

[1]Division of Nuclear Medicine, Ghent University Hospital, Ghent, Belgium; [2]Division of Nuclear Medicine, OLV Hospital, Aalst, Belgium; and [3]Hydraulics Laboratory, Ghent University, Ghent, Belgium

Various automatic algorithms are now being developed to calculate left ventricular (LV) and right ventricular (RV) ejection fraction from tomographic radionuclide ventriculography. We tested the performance of 4 of these algorithms in estimating LV and RV volume and ejection fraction using a dynamic 4-chamber cardiac phantom. **Methods:** We developed a realistic physical, dynamic 4-chamber cardiac phantom and acquired 25 tomographic radionuclide ventriculography images within a wide range of end-diastolic volumes, end-systolic volumes, and stroke volumes. We assessed the ability of 4 algorithms (QBS, QUBE, 4D-MSPECT, and BP-SPECT) to calculate LV and RV volume and ejection fraction. **Results:** For the left ventricle, the correlations between reference and estimated volumes (0.93, 0.93, 0.96, and 0.93 for QBS, QUBE, 4D-MSPECT, and BP-SPECT, respectively; all with $P < 0.001$) and ejection fractions (0.90, 0.93, 0.88, and 0.92, respectively; all with $P < 0.001$) were good, although all algorithms underestimated the volumes (mean difference [±2 SDs] from Bland–Altman analysis: −39.83 ± 43.12 mL, −33.39 ± 38.12 mL, −33.29 ± 40.70 mL, and −16.61 ± 39.64 mL, respectively). The underestimation by QBS, QUBE, and 4D-MSPECT was greater for higher volumes. QBS, QUBE, and BP-SPECT could also be tested for the right ventricle. Correlations were good for the volumes (0.93, 0.95, and 0.97 for QBS, QUBE, and BP-SPECT, respectively; all with $P < 0.001$). In terms of absolute volume estimation, the mean differences (±2 SDs) from Bland–Altman analysis were −41.28 ± 43.66 mL, 11.13 ± 49.26 mL, and −13.11 ± 28.20 mL, respectively. Calculation of RV ejection fraction correlated well with true values (0.84, 0.92, and 0.94, respectively; all with $P < 0.001$), although an overestimation was seen for higher ejection fractions. **Conclusion:** Calculation of LV and RV ejection fraction based on tomographic radionuclide ventriculography was accurate for all tested algorithms. All algorithms underestimated LV volume; estimation of RV volume seemed more difficult, with different results for each algorithm. The more irregular shape and inclusion of a relatively hypokinetic RV outflow tract in the right ventricle seemed to cause the greater difficulty with delineation of the right ventricle, compared with the left ventricle.

Received Jun. 7, 2004; revision accepted Aug. 23, 2004.

For correspondence or reprints contact: Pieter De Bondt, MD, Nuclear Medicine Division, P7, University Hospital Ghent, De Pintelaan 185, 9000 Ghent, Belgium.

E-mail: pdebondt@skynet.be

Key Words: dynamic cardiac model; tomographic radionuclide angiography; validation

J Nucl Med 2005; 46:165–171

The accurate estimation of right ventricular (RV) ejection fraction has been challenging for years. In nuclear medicine, various isotopes and injection techniques have extensively been studied (*1–6*). The first-pass technique of a radioactive bolus through the right heart circulation was often used but became unpopular because its success grossly depends on a perfect bolus injection, introducing operator dependency and limiting the application to experienced people. Planar radionuclide ventriculography for the calculation of RV ejection fraction was not optimal because of the important overlap of atrial with ventricular activity in left anterior oblique views. Tomographic radionuclide ventriculography seems to overcome this problem by offering a 3-dimensional image of the vascular structures of the heart. Initially, software was developed on the basis of manual or semiautomatic contour detection (*4,7*), but these procedures were time consuming, still needed experienced people to process the images, and brought uncertainties about reproducibility. It has become clear that a good algorithm has to be accurate, automatic, and fast. Today, new automatic algorithms such as QBS (*8*), QUBE (*9*), and 4D-MSPECT (*10*) have become available. The validation of these programs is limited to a comparison of left ventricular (LV) ejection fraction from planar radionuclide ventriculography with LV ejection fraction from tomographic radionuclide ventriculography. To our knowledge, validation studies for the calculation of LV and RV volume and RV ejection fraction are lacking. Only 1 program, BP-SPECT (*11*), has validation data for the right ventricle. The aim of this study was, therefore, to test these 4 algorithms using a physical, dynamic 4-chamber cardiac phantom.

MATERIALS AND METHODS

Phantom Description

Our realistic cardiac phantom includes 2 ventricles and 2 atria (Fig. 1). The chamber walls are about 2 mm thick and are made of a silicone elastomer (Wilsor Kunstharsen). The atrioventricular valve plane, however, is made of a membrane 1–2 mm thick. Both ventricles are filled and emptied through the outflow tracts. The atria are filled through tubes connected at the base of the model. The atrioventricular valve plane itself hangs in a polyvinyl chloride ring, which allows the cardiac model to move during the contraction in the long-axis direction. The interventricular septum is constructed from a 15-mm-thick synthetic spongy material. Both ventricles are covered with an external membrane, which makes it possible to achieve septal thickening during end-systole. Because the RV outflow tract is relatively hypokinetic, it has been modeled with a stiff polyvinyl chloride tube. The outflow tract of the RV is responsible for only 15% of the RV stroke volume (*12*), and the amplitude of the RV outflow tract on images of tomographic radionuclide angiography has also been shown to be low (*13*). That study was on patients with Wolff-Parkinson-White syndrome, in which this region in known to have a delay in phase but not necessarily a decrease in amplitude.

Two separate double-acting piston pumps are connected to the cardiac phantom by reinforced acrylic pipes and supply the chamber with water, thereby simulating filling and emptying of the chambers. The ejection of both pumps supplied both ventricles, whereas the suctioning at the other side of the pistons in the pumps emptied both atria. In this way, during the opposite movement both ventricles were emptied and both atria were filled, resulting in the same stroke volume in all 4 cardiac chambers. This stroke volume was easily adjusted by changing the length of the piston (range, 25.74–73.99 mL). An activity of 74 MBq (2 mCi) of ^{99m}Tc per liter of water was used in the chambers, with no background activity. Volume variation in the phantom was sinusoidal.

To set the reference end-systolic volumes in each of the 4 chambers, the pistons were moved to their end-systolic positions. After that, the chamber was emptied and the predefined end-systolic volume was added through a tap on the connecting tubes between the phantom and the pumps. The ranges of volumes and ejection fractions used in this experiment were 51–196 mL for LV end-diastolic volume, 17–162 mL for LV end-systolic volume, 17%–70% for LV ejection fraction, 60–209 mL for RV end-diastolic volume, 26–175 mL for RV end-systolic volume, and 16%–70% for RV ejection fraction.

Data Acquisition

Twenty-five experiments were performed. Tomographic radionuclide ventriculography data were acquired using a 3-head γ-camera (IRIX; Marconi-Phillips) with low-energy high-resolution collimators. The acquisition parameters were as follows: a 360° step-and-shoot rotation, 40 stops per head, 30 s per stop, a 64 × 64 matrix, a zoom of 1.422 (pixel size, 6.5 mm), and 16 time bins per R-R interval, the latter being fixed at 60 beats/min. An R-wave simulator synchronized with the pistons supplied R-wave triggers. Projection data were prefiltered using a Butterworth filter (cutoff frequency, 0.5 cycles/cm; order, 5) and reconstructed by filtered backprojection using a ramp filter. Data were then reoriented into gated short-axis tomograms. The resulting gated short-axis datasets were then used as input for the 4 algorithms.

Data Processing

QBS. QBS (*8*) (Fig. 1B) is primarily a gradient-based method. A deformable ellipsoid is used to approximate the LV endocardium, followed by a sampling (not further clarified) to compute the endocardial surface for each gating interval. This sampling is used to generate a second surface to represent the RV endocardium. A correction is performed to locate the pulmonary valve. The right ventricle and pulmonary artery are separated by truncating the RV surface with a plane. However, how this plane is being positioned during reconstruction is not clear.

QUBE. In the QUBE method (*9*), the LV cavity at end-diastole is delineated by segmentation using an iterative threshold technique. An optimal threshold is reached when the corresponding isocontour best fits the first derivative of the end-diastolic count distribution. This optimal threshold is then applied to delineate the LV cavity on the other time bins. LV volumes are determined with a geometry-based method and are used to calculate the ejection fraction.

4D-MSPECT. 4D-MSPECT (*10*) uses gradient and segmentation operators in conjunction with phase analysis to track the surface contours of the left ventricle through the cardiac cycle. 4D-MSPECT calculates only LV ejection fraction and LV volume. Calculation of RV parameters is not yet available. Currently, only 1 abstract is available about the use of 4D-MSPECT in tomographic radionuclide ventriculography.

BP-SPECT. BP-SPECT (*11*) is based on the use of a threshold obtained from the percentage of maximum counts in each cavity. After maximum activity in the right ventricle is located, the algorithm automatically defines ventricular regions as those pixels with counts ≥ 35% of the threshold of maximum end-diastolic counts over the entire cardiac volume. Biventricular ejection fractions are computed from systolic count changes within voxels inside identified ED and ES ventricular surfaces. All calculations are count based, not geometric. For analyzing the right ventricle, the pulmonary valve plane is defined to be as high as necessary to include all structures shown by the algorithms to have counts that increase synchronously with LV count increases.

Statistical Analysis

χ^2 analysis was used to test whether data were normally distributed. Results are reported as mean ± SD. Correlations (r) between calculated and true (measured) values are expressed as the Pearson correlation coefficient. Variability about the regression line is expressed as the SEE. Bland–Altman analysis of differences between pairs of estimated and reference values was used to search for trends and systematic errors. Statistical significance was defined as $P < 0.05$.

RESULTS

Volume Calculation

All values of both calculated and real ejection fraction and volume were normally distributed. Correlation coefficients between the calculated and real volumes of the left ventricle for QBS, QUBE, 4D-MSPECT, and BP-SPECT were 0.93, 0.93, 0.96, and 0.93, respectively (all with $P <$ 0.001) (Fig. 2). There was a global underestimation of calculated volumes (mean difference ± 2 SDs: −39.83 ± 43.12 mL, −33.39 ± 38.12 mL, −33.29 ± 40.70 mL, and −16.61 ± 39.64 mL for QBS, QUBE, 4D-MSPECT, and

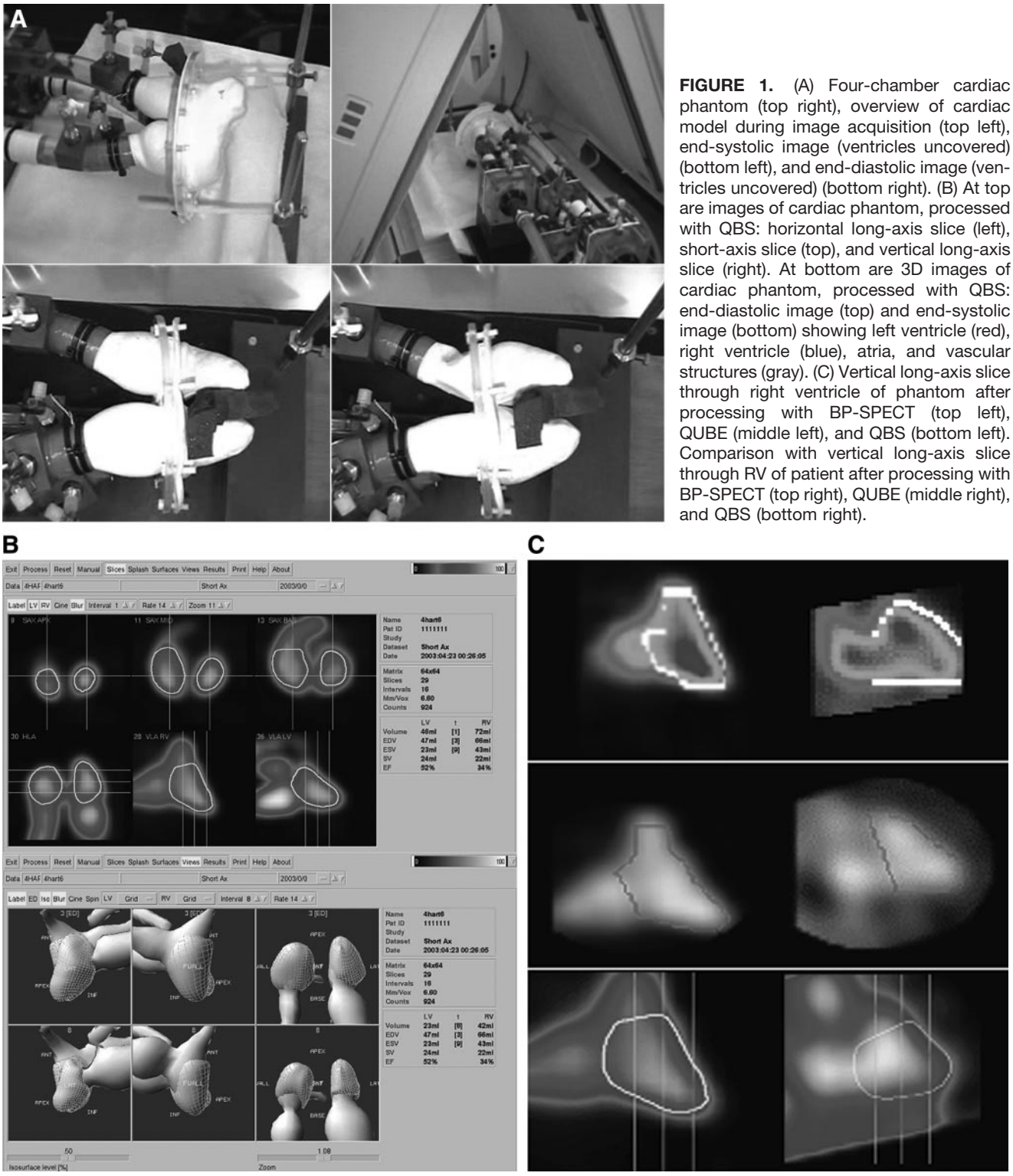

FIGURE 1. (A) Four-chamber cardiac phantom (top right), overview of cardiac model during image acquisition (top left), end-systolic image (ventricles uncovered) (bottom left), and end-diastolic image (ventricles uncovered) (bottom right). (B) At top are images of cardiac phantom, processed with QBS: horizontal long-axis slice (left), short-axis slice (top), and vertical long-axis slice (right). At bottom are 3D images of cardiac phantom, processed with QBS: end-diastolic image (top) and end-systolic image (bottom) showing left ventricle (red), right ventricle (blue), atria, and vascular structures (gray). (C) Vertical long-axis slice through right ventricle of phantom after processing with BP-SPECT (top left), QUBE (middle left), and QBS (bottom left). Comparison with vertical long-axis slice through RV of patient after processing with BP-SPECT (top right), QUBE (middle right), and QBS (bottom right).

BP-SPECT, respectively), and this underestimation increased as volumes increased (slope of the Bland–Altman regression line was significantly different from zero for QBS, QUBE, and 4D-MSPECT). QBS, QUBE, and BP-SPECT were also used to calculate RV volume (Fig. 3). Correlation coefficients between reference and estimated RV volume were within the same range as for the left ventricle (0.93, 0.95, and 0.97 for QBS, QUBE, and BP-SPECT, respectively; all with $P < 0.001$). QBS and BP-SPECT significantly underestimated RV volume (mean difference ± 2 SDs: −41.28 ± 43.66 mL and −13.11 ± 28.20 mL for QBS and BP-SPECT, respectively), whereas QUBE

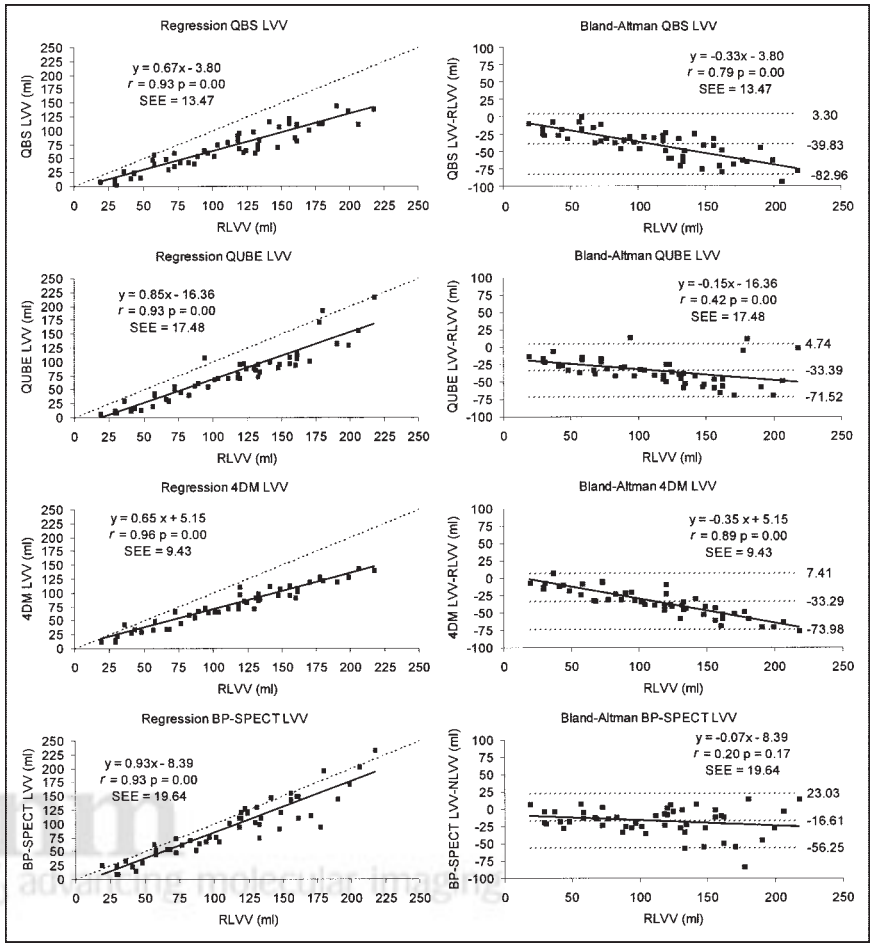

FIGURE 2. Linear regression and Bland–Altman analysis of LV volume calculation (end-diastolic volume and end-systolic volume) for 4 methods (QBS, QUBE, 4D-MSPECT. and BP-SPECT). LVV = LV volume; 4DM = 4D-MSPECT.

significantly overestimated RV volume (mean difference ± 2 SDs: 11.13 ± 49.26 mL). The underestimation of RV volume in QBS and the overestimation of RV volume in QUBE increased with increasing ejection fraction.

Ejection Fraction Calculation

The correlation between the calculated and reference LV ejection fraction for the 4 programs was very acceptable (0.90, 0.93, 0.88, and 0.92 for QBS, QUBE, 4D-MSPECT, and BP-SPECT, respectively; all with $P < 0.001$) (Fig. 4). Mean differences (±2 SDs) were 4.46% ± 20.19%, 3.03% ± 15.94%, −2.72% ± 16.44%, and 0.91% ± 20.16%, respectively, and only the BP-SPECT program showed a significant trend to overestimate the LV ejection fraction with increasing ejection fraction. For RV ejection fraction, good correlations were seen for QUBE and BP-SPECT (0.92 and 0.94, respectively; both with $P < 0.001$) and a slightly lower correlation coefficient was seen for QBS (0.84; $P < 0.001$) (Fig. 5). QBS, QUBE, and BP-SPECT overestimated RV ejection fraction (mean difference ± 2 SDs: 8.08% ± 34.20%, 7.98% ± 26.24%, and 3.67% ± 17.36%, respectively), and this overestimation increased with increasing ejection fraction for all 3 methods.

DISCUSSION

We have demonstrated that QBS, QUBE, 4D-MSPECT, and BP-SPECT accurately calculate LV and RV ejection fraction. All algorithms underestimated LV volume, an observation for which we have no clear explanation. A partial inclusion of atrial activity in the ventricular region could be an explanation but was not visually confirmed. On the contrary, we previously reported an overestimation of LV volume with BP-SPECT, using a biventricular cardiac model (*14*). In that model, however, the left ventricle consisted of double concentric walls (inner and outer walls), mimicking the LV myocardium. For measurement of the exact volume of the left ventricle, the inner wall was suctioned through the entrance at the atrioventricular border, and this situation was not ideal since the outer wall together with the inner wall moved inside during this operation (space between the walls was kept constant) and we could not see whether the left ventricle was perfectly emptied. It is our experience that the 4-chamber model, which is provided with single ventricular walls and an improved pump experimental setup, causes fewer deviations in correct volume measurements. It is also our experience that constructing phantoms to measure absolute parameters (e.g., vol-

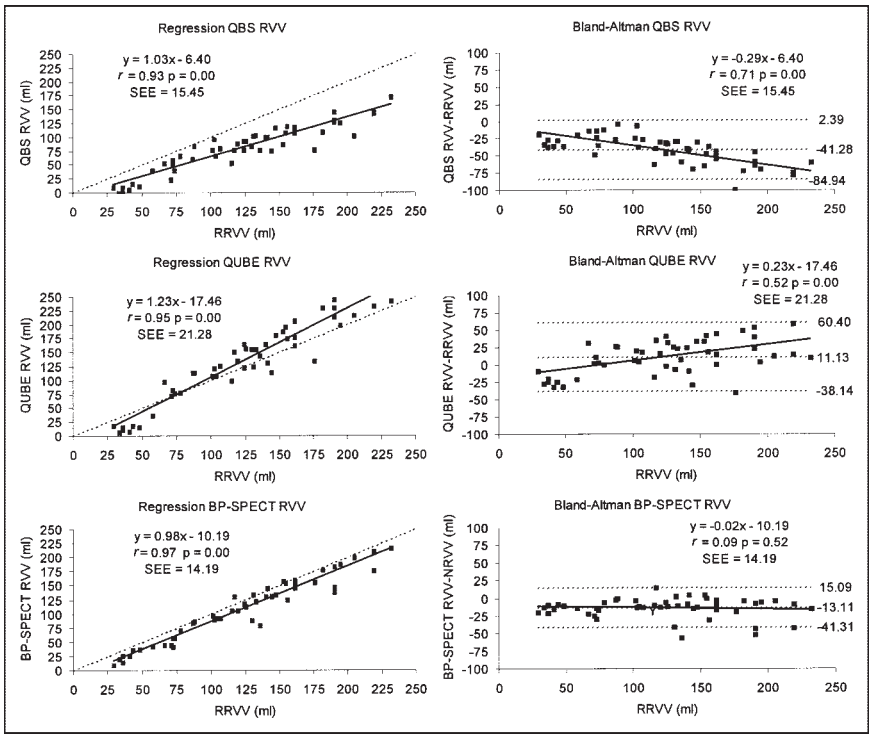

FIGURE 3. Linear regression and Bland–Altman analysis of RV volume calculation (end-diastolic volume and end-systolic volume) for 3 methods (QBS, QUBE, and BP-SPECT). RVV = RV volume.

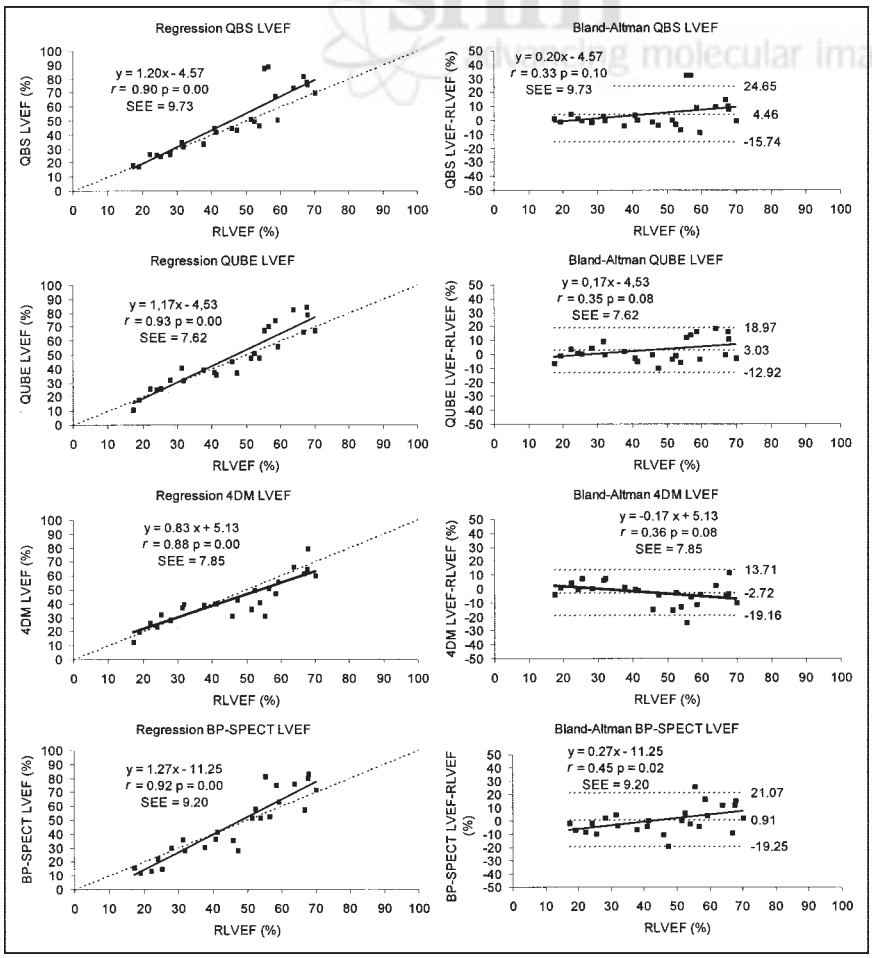

FIGURE 4. Linear regression and Bland–Altman analysis of LV ejection fraction calculation for 4 methods (QBS, QUBE, 4D-MSPECT, and BP-SPECT). LVEF = LV ejection fraction; 4DM = 4D-MSPECT.

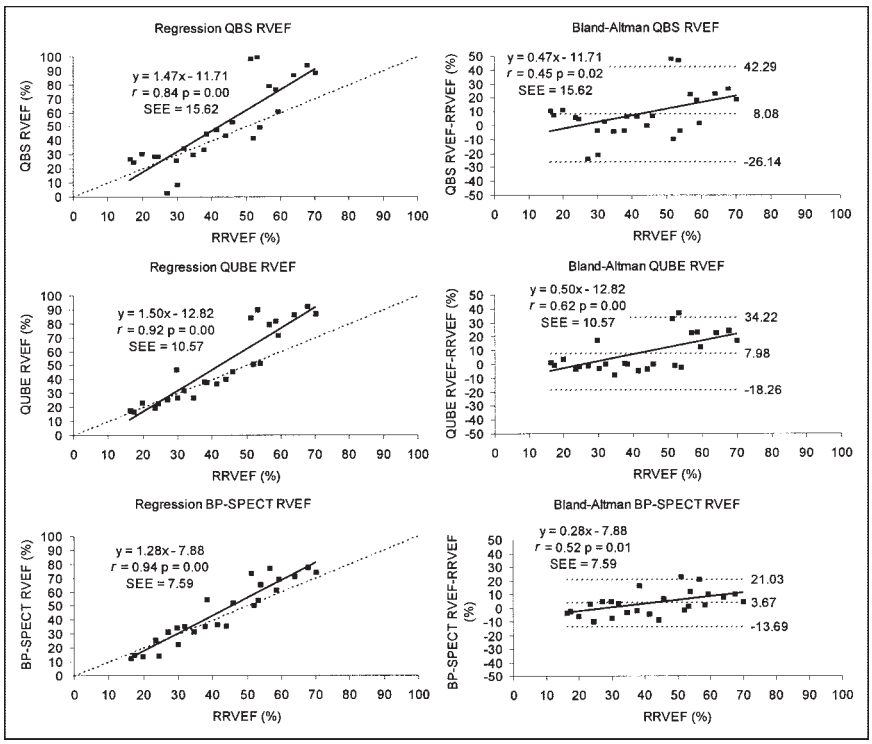

FIGURE 5. Linear regression and Bland–Altman analysis of RV ejection fraction calculation for 3 methods (QBS, QUBE, and BP-SPECT). RVEF = RV ejection fraction.

umes) is far more difficult than constructing phantoms to measure relative parameters (e.g., ejection fraction). All 4 algorithms were developed to calculate volumes in human organs, taking into account the influence of attenuation and scatter from nearby structures. In this paper, as in the previous report, no background activity was used, no scatter or attenuation correction was performed, and no thoracic phantom was used. Because we used an isolated heart phantom, the count threshold differed from that used in human examinations (*14*).

The potential benefit of tomographic radionuclide ventriculography over other routine cardiac imaging modalities is the accurate, fast, and simple measurement of RV volume and RV ejection fraction. The gold standard for these calculations is now MRI. Nevertheless, the MRI procedure and calculations are still time consuming and operator dependent and do not take into account the numerous trabeculae, which turn the endocardium of the right ventricle into a very irregular surface. Unfortunately, our 4-chamber phantom contains ferromagnetic material and could not be tested in the MRI setting. An additional problem with calculating correct RV volumes with tomographic radionuclide ventriculography is the difficulty of delineating the RV outflow tract. This relatively hypokinetic structure contains a part of the volume of the right ventricle but does not really participate in its contraction. Furthermore, exact localization is far more difficult for the pulmonary valve than for the aortic valve.

Little has been published on the validation of tomographic radionuclide ventriculography for calculation of RV volume and RV ejection fraction. To our knowledge, of the 4 tested algorithms, a validation study has been done only for BP-SPECT (*11*). The findings of that study were comparable to ours regarding correlation between MRI and BP-SPECT in the calculation of RV volume and ejection fraction and regarding underestimation of RV volume.

Our results indicate that, compared with QUBE and BP-SPECT, QBS yields a slightly lower correlation coefficient for the calculation of RV ejection fraction and underestimates RV volume. We believe that this is because QBS locates the end of the outflow tract of the right ventricle more toward the apex of the right ventricle (Fig. 1C). For QUBE and BP-SPECT, which calculated more accurate RV volumes, a larger RV volume including distal parts in the RV outflow tract is delineated. Therefore, in manufacturing our model, we paid special attention to forming the distal part of the RV outflow tract from noncompliant PVC tubes, to test whether the software could find the exact border of the right ventricle.

BP-SPECT is the only algorithm showing no significant trend in volume calculations for either the left or the right ventricle. The trend seen with the other algorithms not only is significant but also plays a major role in dilated hearts. Because cardiac volume measurements are important diagnostic and prognostic tools in the workup of cardiovascular disease, BP-SPECT is the method of choice when one needs to report tomographic radionuclide ventriculography findings with volume calculations.

CONCLUSION

We have shown, using a dynamic 4-chamber phantom, that QBS, QUBE, 4D-MSPECT, and BP-SPECT accurately estimate RV and LV ejection fraction. In calculations of RV volumes, the software codes need to take into account the relative hypokinetic RV outflow tract, which has to be included in the RV volume. The more irregular shape of the right ventricle, and the inclusion of a relatively hypokinetic right ventricle outflow tract in the right ventricle, seem to cause the greater difficulty with its delineation, compared with delineation of the left ventricle.

ACKNOWLEDGMENTS

We thank Edward Ficaro, PhD, Ann Arbor Medical Center, for kindly allowing us to use his program (4D-MSPECT) and Philippe Briandet, PhD, SEGAMI Corporation, for making it possible for us to try the program QUBE. Special thanks are extended to Ken Nichols, PhD, Long Island Jewish Medical Center, for advising us during processing with BP-SPECT. One author is funded by a specialization grant from the Institute for the Promotion of Innovation by Science and Technology (IWT 021228).

REFERENCES

1. Franken PR, Delcourt E, Ham HR. Right ventricular ejection fraction: comparison of technetium-99m first pass technique and ECG-gated steady state krypton-81m angiocardiography. *Eur J Nucl Med.* 1986;12:365–368.
2. Gayed I, Boccalandro F, Fang B, Podoloff D. New method for calculating right ventricular ejection fraction using gated myocardial perfusion studies. *Clin Nucl Med.* 2002;27:334–338.
3. Ham HR, Franken PR, Georges B, Delcourt E, Guillaume M, Piepsz A. Evaluation of the accuracy of steady-state krypton-81m method for calculating right ventricular ejection fraction. *J Nucl Med.* 1986;27:593–601.
4. Mariano-Goulart D, Collet H, Kotzki PO, Zanca M, Rossi M. Semi-automatic segmentation of gated blood pool emission tomographic images by watersheds: application to the determination of right and left ejection fractions. *Eur J Nucl Med.* 1998;25:1300–1307.
5. Oliver RM, Fleming JS, Dawkins KD, Waller DG. Right ventricular function at rest and during submaximal exercise assessed by 81Krm equilibrium ventriculography in normal subjects. *Nucl Med Commun.* 1993;14:36–40.
6. Perings SM, Perings C, Kelm M, Strauer BE. Comparative evaluation of thermodilution and gated blood pool method for determination of right ventricular ejection fraction at rest and during exercise. *Cardiology.* 2001;95:161–163.
7. Groch MW, Marshall RC, Erwin WD, Schippers DJ, Barnett CA, Leidholdt EM Jr. Quantitative gated blood pool SPECT for the assessment of coronary artery disease at rest. *J Nucl Cardiol.* 1998;5:567–573.
8. Van Kriekinge SD, Berman DS, Germano G. Automatic quantification of left ventricular ejection fraction from gated blood pool SPECT. *J Nucl Cardiol.* 1999;6:498–506.
9. Vanhove C, Franken PR, Defrise M, Momen A, Everaert H, Bossuyt A. Automatic determination of left ventricular ejection fraction from gated blood-pool tomography. *J Nucl Med.* 2001;42:401–407.
10. Ficaro EP, Quaife RF, Kritzman JN, Corbett JR. Validation of a new fully automatic algorithm for quantification of gated blood pool SPECT: correlations with planar gated blood pool and perfusion SPECT [abstract]. *J Nucl Med.* 2002;43(suppl):97P.
11. Nichols K, Saouaf R, Ababneh AA, et al. Validation of SPECT equilibrium radionuclide angiographic right ventricular parameters by cardiac magnetic resonance imaging. *J Nucl Cardiol.* 2002;9:153–160.
12. Geva T, Powell AJ, Crawford EC, Chung T, Colan SD. Evaluation of regional differences in right ventricular systolic function by acoustic quantification echocardiography and cine magnetic resonance imaging. *Circulation.* 1998;98:339–345.
13. Nakajima K, Bunko H, Tada A, et al. Nuclear tomographic phase analysis: localization of accessory conduction pathway in patients with Wolff-Parkinson-White syndrome. *Am Heart J.* 1985;109:809–815.
14. De Bondt P, Nichols K, Vandenberghe S, et al. Validation of gated blood-pool SPECT cardiac measurements tested using a biventricular dynamic physical phantom. *J Nucl Med.* 2003;44:967–972.